Desalination and Water Treatment
www.deswater.com

doi:10.5004/dwt.2021.27243

226 (2021) 362–371
June

Discoloration and mineralization of Direct Orange 39 textile dye in water by atmospheric plasma and ferrous ion

César Torres Segundo[a], Josefina Vergara Sánchez[a,*], Esteban Montiel Palacios[a], Aarón Gómez Díaz[b], Pedro Guillermo Reyes Romero[b], Horacio Martínez Valencia[c]

[a]*Laboratorio de Análisis y Sustentabilidad Ambiental, Escuela de Estudios Superiores de Xalostoc, Universidad Autónoma del Estado de Morelos, Xalostoc, Ayala, Morelos, C.P. 62715, México, emails: vergara@uaem.mx (J.V. Sánchez), cesar.torres@uaem.mx (C.T. Segundo), esteban.montiel@uaem.mx (E.M. Palacios)*
[b]*Laboratorio de Física Avanzada, Facultad de Ciencias, Universidad Autónoma del Estado de México, Instituto Literario No. 100 Col. Centro, Toluca, Estado de México, C.P. 50000, México, emails: agomezd@uaemex.mx (A.G. Díaz), pgrr@uaemex.mx (P.G.R. Romero)*
[c]*Laboratorio de Espectroscopia, Instituto de Ciencias Físicas, Universidad Nacional Autónoma de México, A.P. 48-3, Cuernavaca, Morelos, C.P. 62251, México, email: hm@icf.unam.mx (H.M. Valencia)*

Received 24 October 2020; Accepted 19 March 2021

ABSTRACT

The wastewater generated by the textile industry causes serious problems for ecosystems when discarded without effective treatment. Samples of water contaminated with the Direct Orange 39 dye were treated by plasma discharge generated at atmospheric pressure for 150 min. In this study, the initial concentration of the dye was 1.0 mM with an initial volume of 250 mL. Moreover, iron filings (Fe^{2+}) were used as a catalyst. Reduction of the dye concentration in the samples was possible as a function of treatment time. This was verified by the absorbance spectrum in the UV-vis range. During treatment, every 15 min, we monitored the electric current, voltage, temperature of the water containing the dye, volume, pH, electrical conductivity, absorbance, concentrations of nitrates and nitrites, total organic carbon (TOC), chemical oxygen demand (COD), and the optical emission spectrum of the plasma and determined the dye concentration, discoloration factor, percentage of mineralization, and G_{50} (which expresses the amount of energy required to eliminate 50% of the pollutant), and electrical cost. Results showed that the efficiency of the dye degradation by plasma is a function of treatment time, and we obtained the removal of 50% of the colorant in 34 min and 94.2% in 120 min; additionally, COD was at 98.6%, the TOC was at 98.7%, and the percentage of mineralization was at 98.5% after 150 min of treatment. The maximum concentrations of nitrates and nitrites were 214 and 32 mg/L, respectively, after 150 min. From the optical spectrum of plasma emission, different species were identified (e.g., OH, N_2, Na, H_α, and H_β). The G_{50} value was 0.825 g/kWh, and the electrical cost calculated for the treatment of 1 m^3 of water with this colorant using plasma was $3.20 after 150 min of treatment.

Keywords: Plasma; Textile dye; Total organic carbon; Chemical oxygen demand; Optical emission spectroscopy

1. Introduction

Water is vital for the vivification of the planet [1]. However, the increasing degree of industrialization worldwide and the excessive use of chemical products or their derivatives have led to a gradual increase in the number of unwanted contaminants in drinking water sources [2]. Dyes are considered one of the major pollutants in wastewater [3]. Most countries are currently aware of the importance of proper treatment of wastewater that contain dyes because ~17%–20% of industrial wastewater originates from the textile, leather, paint, and paper industries. Furthermore, more than 300,000 tons/y are drained into streams from the textile

* Corresponding author.

1944-3994/1944-3986 © 2021 Desalination Publications. All rights reserved.

industry and other industries [4]. Even a small amount of dye in water (e.g., 5–20 mg/L) is noticeable because it affects the transparency of the water [5]. Direct acid and reactive dyes are anionic, whereas basic dyes are cationic. The highest toxicity levels have been found for basic and direct dyes [6]. Direct dyes (e.g., DO39) are widely used for cotton dyeing owing to their ease of use and low cost [7].

Generally, the most widely used methods for removing dye from water can be divided into three categories: chemical methods (advanced oxidation processes (AOPs), e.g., the Fenton process [8], ozonation [9], and photochemical and electrochemical [10]), physical treatment (e.g., adsorption [11], membrane separation [12], flocculation [13], and plasma [14]), and biological treatment [15]. Recently, the application of atmospheric plasma to the surface of water with dye has been demonstrated as an efficient alternative for the degradation of these contaminants, which does not require the addition of chemical products. It has been reported that in this treatment, $^{\bullet}OH$, $^{\bullet}H$, $^{\bullet}O$, $HO_2^{\bullet}$, $O_2^{\bullet-}$, H_2O_2, and O_3 are generated among other species, which are capable of degrading these pollutants [16,17]. Among these chemical species, H_2O_2 and OH are the most efficient in the organic matter removal. Additionally, the system produces plasma-induced UV irradiation and reactive species (RS), including reactive oxygen species (ROS) and reactive nitrogen species (RNS) [18]. Specifically, H_2O_2 and nitrate ions (NO_3^-) can be generated by plasma in a liquid using an electric discharge [19]. The study of real samples of water contaminated with dye is very interesting, however, the study of model samples treated with plasma at atmospheric pressure is still important, because there is no complete understanding of the fate of the products intermediates and that in general, the production of unwanted products should be avoided. To better understand these complex processes, it is important that the models consider not only the relevant chemistry, but also the dynamic effects of the fluids and the characteristics of the plasma used.

This study generally aims to examine the application of an electrical discharge (i.e., corona type) during the degradation of DO39 dye. The atmospheric plasma was formed at the liquid–air interface to treat water samples with textile dye. This study combined physical treatment (plasma) with chemical effects using the catalyst (Fe^{2+}) to provide similarity to the Fenton process. During treatment, the following physical and chemical parameters were monitored: electric current, voltage, temperature of the water containing the dye, volume, pH, electrical conductivity, absorbance, concentrations of nitrates and nitrites, total organic carbon (TOC), chemical oxygen demand (COD), and the optical emission spectrum of the plasma. We determined the dye concentration, discoloration factor, percentage of mineralization, G_{50} (which expresses the amount of energy required to eliminate 50% of the pollutant), and electrical cost. The experiment were performed in the Laboratorio de Análisis y Sustentabilidad Ambiental of the Universidad Autónoma del Estado de Morelos.

2. Methodology

2.1. Experimental system

Plasma treatment at atmospheric pressure of a solution with the DO39 dye was performed in an acrylic reactor (batch-type reactor), which had a container for treatment inside (Fig. 1) that was made of Pyrex glass with a capacity of 400 mL and included two 3 mm-diameter tungsten electrodes that were aligned with each other; the cathode was immersed in the dye solution (1.0 cm inside), and the anode was placed on the solution surface at a 3 mm distance. The container was fitted with an optical fiber, which allowed it to connect to a spectrometer (StellarNet EPP2000, wavelength range of 200–1,100 nm) to obtain the optical emission spectroscopy (OES) in real time. The plasma was generated on the surface of the solution with a DC source (HP Mod. 6525A, 4.0 kV–50 mA) at a constant power of 80 W.

The DO39 dye was dissolved in water in a 250 mL graduated flask with an initial concentration of 1.0 mM. The dye and iron filings were mixed in the reactor. A Hach HQ40d potentiometer (United States) was used to perform the pH and electrical conductivity measurements. Additionally, a Hach DR3900 spectrophotometer (United States) was used to measure the absorbance in the range of 320–800 nm and to determine nitrate and nitrite concentrations using Hach vials (United States). The discoloration factor was obtained as a function of treatment time with the plasma. Moreover, the TOC and COD were determined using the Hach method (United States) with low-ranking reagents. Sampling was performed every 15 min.

2.2. Preparation of the DO39 solution

DO39 is a recalcitrant compound, and its metabolites can be very toxic to aquatic life [20]. It is mainly used in cloth dyeing, printing, and leather and paper shading. The DO39 dye has a molecular weight of 299.28 g/mol, CAS number of 1325-54-8, color index of 40215, and chemical formula of $C_{12}N_3H_{10}SO_3Na$ (Table 1).

The DO39 dye was weighed on an analytical balance and dissolved in distilled water in a beaker. The solution was placed in a volumetric flask. Iron filings (Fe^{2+}) were added, and the volume was adjusted to 250 mL. The initial solution contained 1.0 mM of DO39 and 1.0 mM of iron filings. A Hach HQ40d multiparameter (United States)

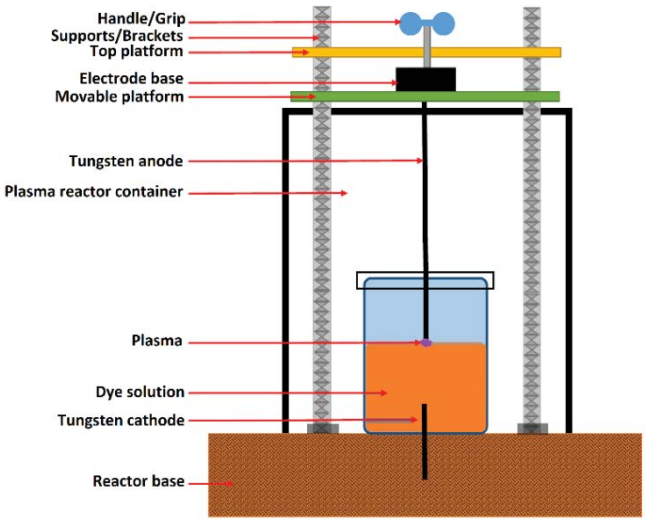

Fig. 1. Batch reactor.

Table 1
Chemical structure of the Direct Orange 39 (DO39) azo dye [21,22]

Structures	Characteristics	Reference
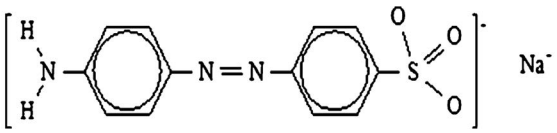	Color index name	Direct Orange 39
	Chemical formula	$C_{12}H_{10}N_3O_3SNa$
	Appearance	Orange powder
	Color index number	40215
	λ_{max} (nm)	444
	Molecular weight (g/mol)	299.28
	CAS number	1325-54-8

was used to measure the pH, electrical conductivity, and temperature. The initial temperature was 25°C, the initial pH was 8.22, and initial electrical conductivity was 260 μS/cm. A Hach DR3900 spectrophotometer (United States) was used to measure the initial absorbance of the DO39 dye solution. Specifically, 1.0 mL of the dye solution was obtained, diluted with 2.0 mL of distilled water, and placed in a quartz cell. The sample was measured using a spectrophotometer. In this case, the characteristic absorbance peak was at 444 nm. To employ spectrophotometry as an analytical technique using the Beer–Lambert law, the dye calibration curve was obtained. This allowed the adjustment equation that related absorbance and solution concentration to be obtained. The analysis was performed every 15 for 150 min. All solutions were made from analytical-grade chemicals, and the experiment was performed five times under the same initial conditions.

2.3. Analysis methods

2.3.1. Discoloration factor

For the analysis of the dye degradation process, the discoloration factor, F_D, was calculated using the following equation [23]:

$$F_D = \frac{\text{Abs}_i - \text{Abs}_t}{\text{Abs}_i}, \tag{1}$$

where Abs_i denotes the measured initial absorbance of the dye solution and Abs_t denotes the measured absorbance at each time interval of the plasma treatment. The temporal development (every 15 min) of the F_D factor was also measured.

2.3.2. Percentage of mineralization

The mineralization of DO39 in the aqueous solution during the atmospheric plasma treatment was monitored by determining the TOC by the Hach method (United States) using low-range vials. The TOC concentration includes the carbon content of the organic dye and other organic intermediate compounds, which were generated during the plasma treatment. A UV-vis spectrophotometer (Hach, DR3900, United States) was used to determine the TOC. The percentage of mineralization was calculated using the following equation [24]:

$$\text{\% of mineralization} = \frac{\text{TOC}_0 - \text{TOC}_F}{\text{TOC}_0} \times 100\% \tag{2}$$

2.3.3. Energy efficiency (G_{50})

The energy efficiency of the degradation process was calculated in terms of the G_{50} constant. This constant expresses the amount of energy required to eliminate 50% of the contaminant. Its equation is as follows [25]:

$$G_{50} = 1.8 \times 10^6 \frac{C_0 V_0 M}{P t_{50}} \tag{3}$$

where C_0 denotes the initial molar concentration of the pollutant at $t = 0$, V_0 is the initial volume of the solution treated in L, M is the molecular weight of the pollutant, P is the electrical power in W, and t_{50} is the time in seconds required to eliminate 50% of the contaminant. The G_{50} factor is expressed in g/kWh.

2.4. Plasma characterization

2.4.1. Optical emission spectroscopy

OES was analyzed when the atmospheric plasma was generated on the surface of the solution. This analysis was conducted using an optical fiber, which passed through the sample container and was located in front of the place where the luminescence was produced. This configuration allowed the direct measurement of the entire luminescence in real time using a StellarNet EPP2000 spectrometer. The spectrometer was operated in the wavelength range of 200–1,100 nm with an integration time of 1,000 ms, and five samples were averaged to collect the spectra. The emission spectra were qualitatively analyzed to assign chemical species to the peaks. To describe the atmospheric plasma used for the treatment, the electron temperature and electron density can be calculated using the intensities of several spectral lines, assuming that the population of the emitting levels follows the Boltzmann distribution [26] and considering that the system has a local thermodynamic equilibrium in some small fraction of this. The following expression were used to calculate the electron temperature:

$$T_e = \frac{E_m(2) - E_m(1)}{k} \left[\ln\left(\frac{I_1 \lambda_1 g_m(2) A_m(2)}{I_2 \lambda_2 g_m(1) A_m(1)} \right) \right]^{-1} \tag{4}$$

where $E_m(i)$ denotes the energy of the upper levels of the lines, k is the Boltzmann constant, $g_m(i)$ represents the statistical weights of the upper levels, and $A_m(i)$ represents their corresponding transition probabilities. These values were obtained from the NIST atomic spectra database lines [27]. I_1 and I_2 denote the relative line intensities in questions, and λ_1 and λ_2 denote the wavelengths of the lines, which were experimentally measured. Using the value of T_e, the value of the electron density of the plasma used during the treatment could also be obtained. Electrons are responsible for most processes in the corona discharge (i.e., ionization, dissociation, and recombination processes) with water molecules. In this study, the following Saha–Boltzmann equation was used to calculate the electron density:

$$n_e = 6\times10^{21}\left(T_e\right)^{\frac{3}{2}}\left(\exp\left[-\frac{E_i}{kT_e}\right]\right) \tag{5}$$

where T_e denotes the electron temperature, E_i is the ionization energy of the species, and k is the Boltzmann constant [28–30].

3. Results

The respective calibration curve was obtained using solutions of known concentrations of the studied DO39 dye (Fig. 2a); the calibration curve was linear and had a high correlation coefficient (R^2 = 0.999). From the calibration curve, the DO39 concentrations during the treatment were calculated.

Fig. 2b presents the calibration curve of DO39, where the red line indicates the mathematical adjustment to a straight line, whose adjustment equation is as follows:

$$y = 0.04933 + \left(4.195\right)x \tag{6}$$

This equation relates the value of absorbance to the dye concentration in the solution as follows:

$$\text{Dye concentration} = \frac{\text{Absorbance} - 0.04933}{4.195} \tag{7}$$

The initial values of pH and the electrical conductivity of the solution were 8.22 and 260 μS/cm, respectively. However, after 150 min, the final values were 2.68 and 630 μS/cm. Generally, during the treatment, a 67.4% decrease in the pH value, and a 2.4-fold increase in the conductivity value were observed for the solution. The decrease in pH resulted from the increasing concentration of H^+, which led to an increase in the conductivity of the solution simultaneously. These changes were the same as those observed in a previous study [31].

The pH value in the solution rapidly decreased during the first 60 min (Fig. 3) owing to the dissociation of water molecules that were in contact with the plasma at atmospheric pressure [3]:

$$H_2O^+_{gas} + nH_2O \rightarrow nH_2O^+ + \left(n-1\right)H^\bullet + nOH^\bullet \tag{8}$$

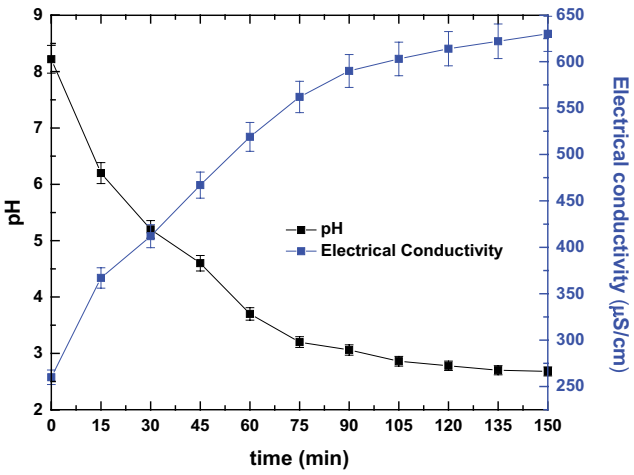

Fig. 3. pH and electrical conductivity of the solution with DO39 during the plasma treatment.

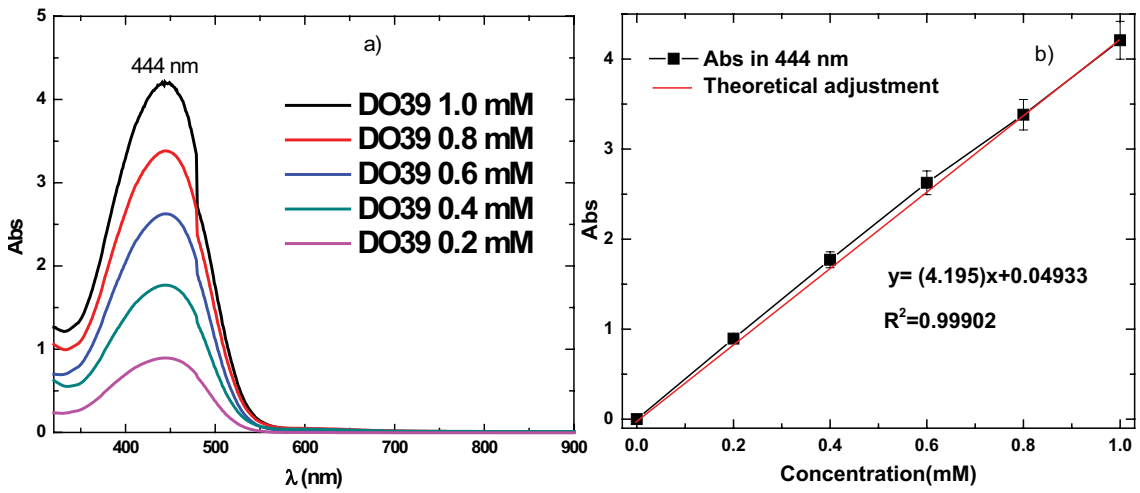

Fig. 2. Direct Orange 39 dye calibration curve: (a) absorbance as a function of known concentration and (b) calibration curve.

With an increase in treatment time, other RS were generated in the solution (ROS and RNS), and some organic acids were produced and contributed to the decrease in pH, which is shown in Fig. 4. Specifically, NO_2^- and NO_3^- were formed in the plasma-treated water via the dissolution of nitrogen oxides formed in the plasma via gas-phase reactions of dissociated N_2 and O_2 or H_2O; this behavior was also observed by Zhou et al. [32].

Fig. 4 shows that nitrates were formed in water at a constant growth rate during the first 30 min, and the concentration was almost constant during the rest of the treatment; the initial value before starting the treatment was zero, which indicated that the presence of these compounds was directly related to the plasma treatment.

With an increase in the time of plasma exposure, the concentration of OH increased, and the possible OH formation is described by the following equations (Eqs. (9)–(11)):

$$H_2O + e^- \rightarrow H^\bullet + OH^\bullet + e^- \quad (9)$$

$$OH^\bullet + OH^\bullet \rightarrow H_2O_2 \quad (10)$$

$$e^- + H_2O_2 \rightarrow OH^- + OH^\bullet \quad (11)$$

Generally, when interacting with OH, the dye begins to degrade into simpler compounds (intermediates), as shown in Eq. (12), which further interacted with OH and reached mineralization, as expressed using Eq. (13).

$$\text{dye DO39} + OH^\bullet \rightarrow \text{Intermediates} \quad (12)$$

$$\text{Intermediates} + OH^\bullet \rightarrow CO_2 + H_2O \quad (13)$$

This study involved the combination of atmospheric plasma processes and the Fenton reaction and assumed that H_2O_2 was generated when plasma interacts with water. When iron (Fe^{2+}) filings were introduced into the dye solution, Fenton-type reactions occurred in the system and thus improved the removal efficiency of the dye present in the water. When Fe^{2+} was added to the solution for organic oxidation, it was directly involved in the catalytic composition of H_2O_2 into OH, as expressed by Eq. (14), whereas Fe^{3+} as the Fenton regent source was initially transformed into Fe^{2+} and consumed large quantities of plasma generated H_2O_2, as expressed by Eq. (15).

$$H_2O_2 + Fe^{2+} \rightarrow OH^\bullet + OH^- + Fe^{3+} \quad (14)$$

$$H_2O_2 + Fe^{3+} \rightarrow H^+ + Fe^{2+} + HO_2^\bullet \quad (15)$$

Compared with AC plasma systems, DC plasmas provide more desirable conditions for Fenton reactions owing to their higher H_2O_2 yields, thus significantly reducing contaminants [33].

Fig. 5 presents the absorption spectra of the solution obtained at different times. The characteristic absorption peak of the DO39 dye occurs at 444 nm, which gradually decreases due to the treatment. After 150 min of applying the corona discharge to the solution, the absorbance (at this wavelength) decreased by more than 98%. This was attributed to the disruption of the chromophore group of the dye molecules. At the end of the treatment, there were compounds that absorbed radiation at wavelengths below 450 nm, which were by-products of the dye mineralization process.

The F_D values were obtained using Eq. (1). Fig. 6A presents the discoloration factor, F_D, determined for the organic compound (DO39) as a function of exposure time to the corona discharge and the catalyst. The discoloration factor, F_D, of DO39 after 150 min of treatment was 0.987. Similarly, using Eq. (7), the concentration of the treated solution could be calculated every 15 min; the behavior of the concentration of the dye in the solution is presented in Fig. 6B. The concentration has a tendency similar to an exponential decay function, and the behavior can be described using the following differential equation (Eq. (16)):

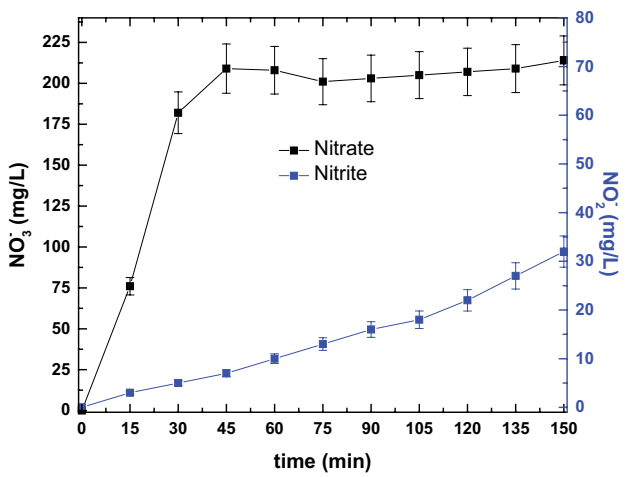

Fig. 4. Nitrate and nitrite concentrations in the solution during plasma treatment.

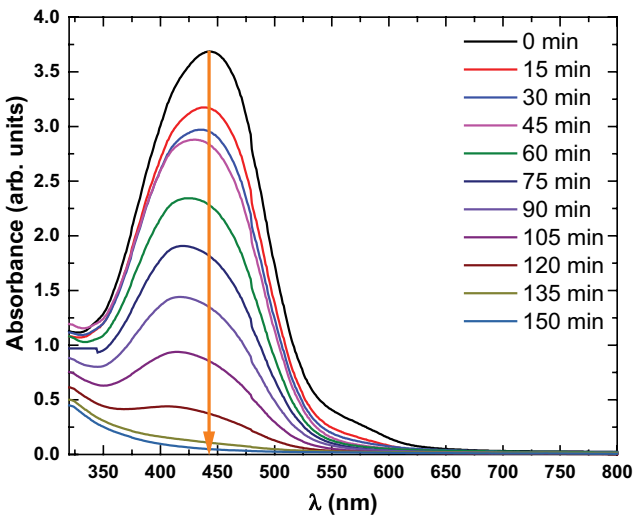

Fig. 5. Absorption spectra as a function of treatment time.

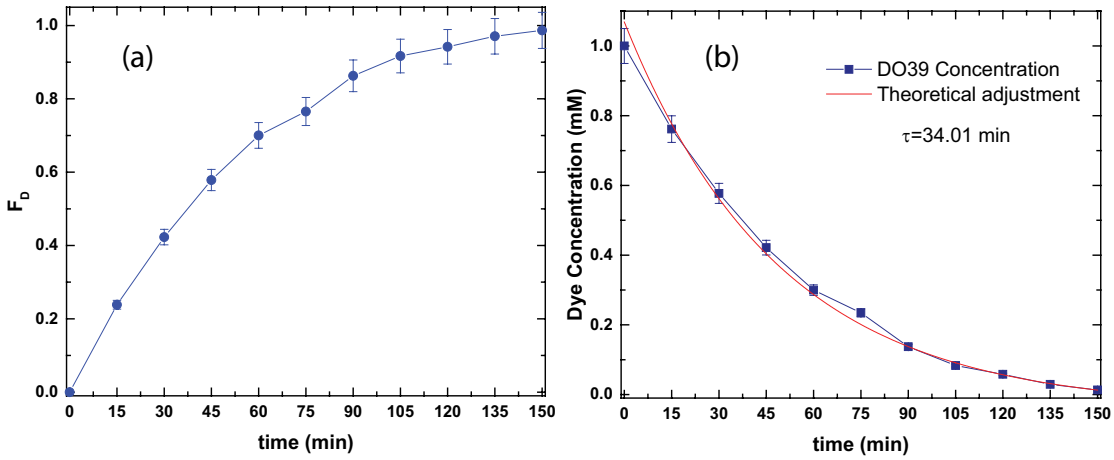

Fig. 6. DO39 degradation with plasma in terms of F_D and dye concentration vs. treatment time with atmospheric plasma: (a) Discoloration factor vs. treatment time and (b) DO39 concentration.

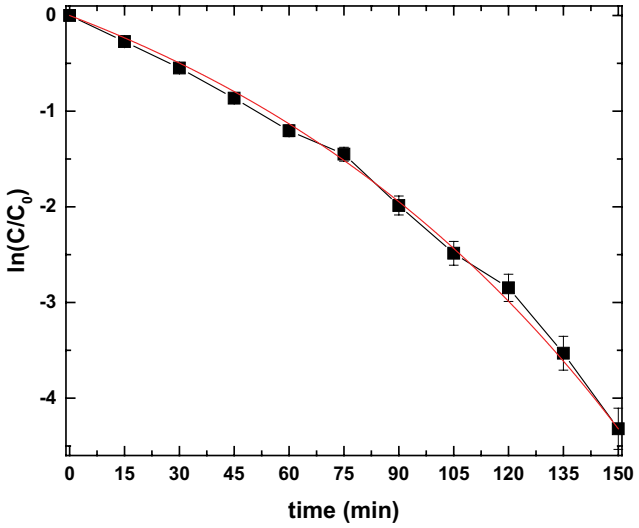

Fig. 7. DO39 degradation.

$$\frac{dC}{dt} = -kC \tag{16}$$

where C denotes the concentration of the dye in the solution, k is the decay constant (degradation rate), and t is the treatment time.

Fig. 7 shows that during the treatment with atmospheric plasma, the concentration of DO39 dye in the solution decreased with time, and the degradation process followed first-order kinetics. The constant rate was calculated using the following equation [24,34]:

$$\ln\left(\frac{C}{C_0}\right) = -kt, \tag{17}$$

where C_0, C, and t denote the initial and final dye concentrations and time, respectively. The values of the first-order rate constant (k) and R^2 values were 0.01546 and 0.97463, respectively.

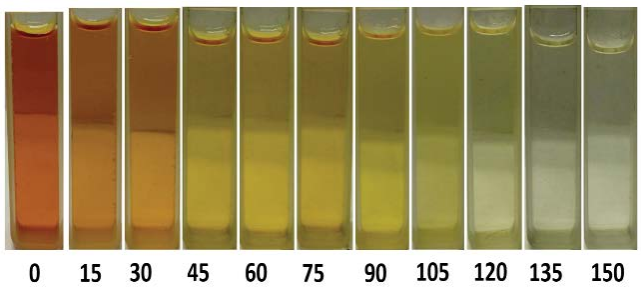

Fig. 8. Discoloration of the solution containing the DO39 dye.

Fig. 8 presents the discoloration of the solution as a function of the time of plasma exposure. This Fig. 8 shows that the initial solution had an orange color; at 15 min, the color intensity decreased; at 45 min, the color changed to yellow; at 105 min, the color was still slightly yellow; and after 135 min, the solution was colorless. This discoloration was attributed to the breaking of the bonds of the chromophore group.

Fig. 9 presents the behaviors of the TOC and COD for the DO39 dye vs. treatment time. The initial values of the TOC and COD were 144 and 88 mg/L, respectively. After 150 min of treatment, these same parameters were 6.3 and 2.9 mg/L, respectively. The COD results indicated that 96% of the dye was transformed into carbon dioxide and water (i.e., it was mineralized). The COD indicated that the water quality significantly improved with treatment because 97% of the organic matter was removed.

Using Eq. (2), the values of the mineralization percentage of the DO39 dye were obtained; these values are presented in Fig. 10. The growth rates in the first 15, 30, and 45 min were 23.8%, 18.4%, and 16.6%, respectively. Additionally, in the first 60 min, there was mineralization of 70.03%. However, treatment of at least 105 min was required to achieve a percentage of mineralization greater than 90%.

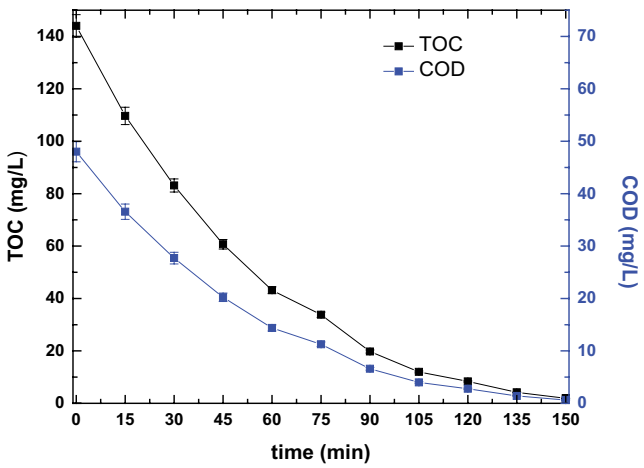

Fig. 9. COD and TOC vs. treatment time.

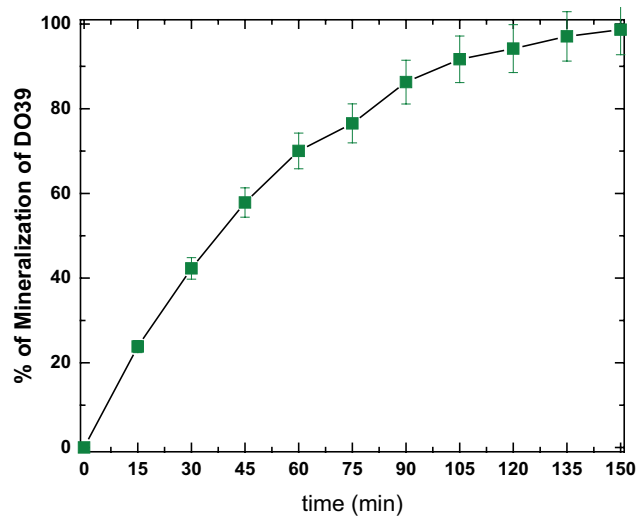

Fig. 10. Percentage of mineralization of DO39 with plasma vs. treatment time.

Fig. 11 shows the OES of the plasma generated compared for distilled water, water–dye, and water–dye–catalyst. The characteristic OH bands were higher when the catalyst (Fe^{2+}) was added. This may be attributed to the presence of iron filings in the solution, which favors OH production.

OES was performed to identify the species generated by the atmospheric plasma, and Fig. 11 presents the emission spectrum between 200 and 1,100 nm obtained from the atmospheric plasma; this technique revealed that most peaks were in the near-UV region (250–400 nm). N_2 bands of the second positive system ($C^3\Pi_u$–$B^3\Pi_g$) at 337.0, 357.5, and 375.5 nm were identified. It was also possible to identify the characteristic doublet of sodium at 590 nm in the spectra with pollutant (D-lines). For both treatments, the band with the highest intensity belongs to OH at 309.5 nm ($A^2\Sigma^+ \rightarrow X^2\Pi$). Additionally, H_α (656.5 nm) and H_β (487.0 nm) were observed and had a low intensity; emissions from singlet O* occurred 777 nm due to the $3p^5P \rightarrow 3s^5S$ transition [27].

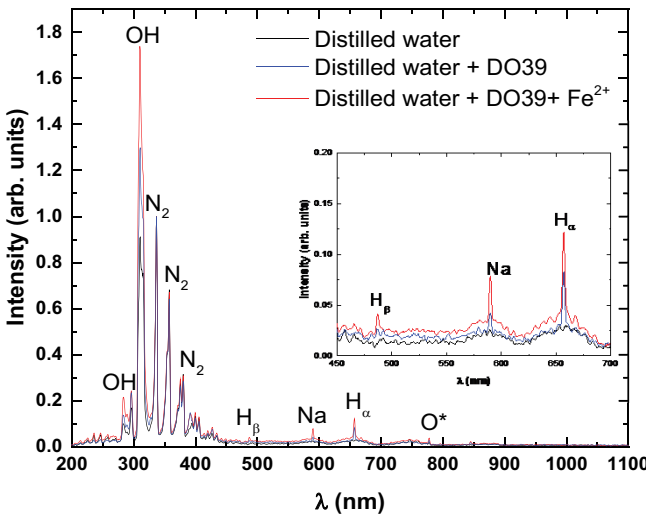

Fig. 11. Optical emission spectra of the corona discharge.

Some of the reactions that occurred in atmospheric plasma and were identified in OES are as follows [35]:

$$e^- + N_2 \rightarrow N_2^* + e^- \quad (18)$$

$$e^- + N_2 \rightarrow N^\bullet + N^\bullet + e^- \quad (19)$$

$$e^- + O_2 \rightarrow O^\bullet + O^\bullet + e^- \quad (20)$$

$$e^- + O_2 \rightarrow O_2^+ + 2e^- \quad (21)$$

$$e^- + O_2 + M \rightarrow O_2^- + M \quad (22)$$

where Eq. (18) expresses the excitation process, Eqs. (19) and (20) show an example of the dissociation process, Eq. (21) shows the ionization of oxygen molecules, and Eq. (22) expresses the electron capture, where M is the third collision partner, which may be O_2 or N_2. All reactions were of high-energy electrons in the atmospheric plasma in air. Electron temperature is a parameter that characterizes the plasma applied for dye treatment; to determine the electron temperature of the applied plasma, the values of H_α and H_β were considered and substituted in Eq. (4), which yielded 6.7 eV for DO39. Using the value obtained from the electron temperature and hydrogen ionization energy and substituting it in Eq. (5), the electron density of the plasma was found to be 6.68×10^{13} particles/cm^3 for DO39. The values obtained in this study are similar to those reported in the literature for plasma at atmospheric pressure. Moreover, the electron density was ~10^{14} cm^{-3}, and the electron temperature was in the range of 1–10 eV [36].

The value of the variable G_{50} was calculated using Eq. (3). In this study, the values of the variables were as follows: initial colorant concentration at C_0 = 0.0001 M, initial volume at V_0 = 0.25 L, M = 299.28 g/mol, electric power at P = 80 W, and time at t_{50} = 2040.6 s. These values, when substituted into the equation, yielded a value for G_{50} of

0.825 g/kWh. This value is similar to those reported in the literature [25]. For example, with a similar initial concentration, for methyl orange, the G_{50} value was 0.45 g/kWh [1]. The structure of methyl orange is very similar to that of DO39. During plasma treatment, the obtained parameters were different; the energy efficiencies of three pulsed discharge modes for Rhodamine B were 0.025 g/kWh, 0.080, and 0.160 g/kWh for streamer discharge, spark discharge, and spark–streamer mixed discharge modes, respectively [23]; for methyl orange G_{50}, with a similar plasma reactor, the value was 0.024 g/kWh [35]; using the batch-type reactor and the described conditions, the DO39 dye could be degraded in a short period of time compared to other studies that used the same dye using PVA-immobilized microorganisms [37]. In previous studies under similar conditions [38], the concentration of hydrogen peroxide produced after plasma treatment was a few mg/L, which indicated that treatment with this type of atmospheric DC plasma produced a sufficient amount of hydrogen peroxide that interacted with iron and accelerated the treatment. The presence of RNS in the plasma-treated solution allows us to propose the use of water in the germination of seeds of agricultural interest in future studies, which has been described by Sivachandiran and Khacef [39]. Iron filings can be recovered by filtration at the end of the treatment, which represents an advantage compared with other processes, such as the Fenton reaction.

One important parameter to consider is the economic cost of the treatment. In this work, only the electric consumption was of relevance because we could ignore, for example, the electrode wear costs because, given that no electrolysis was involved, there was minimal wear during this study. Therefore, the electric cost could be calculated according to Eq. (23) [40]:

$$\text{Electrical cost} = a \times \frac{U \times I \times t_{\text{treatment}}}{v} \tag{23}$$

where U is the voltage discharge (V), I is the current (A), $t_{\text{treatment}}$ is the time needed to degrade the sample (h), v is the volume of the sample (m^3), and a is related to the cost in USD/kWh (0.04 USD/kWh in Mexico). Given a current of 80 mA, a discharge voltage of 1.0 kV, and a volume of 250 mL, the related costs were calculated, as shown in Table 2, in accordance with the treatment time.

The use of chemical agents during the treatment of water that has organic contaminants increases the cost substantially, and this occurs in other AOPs, where an iron sulfate catalyst is used in acid solution. In this study, 250 mL of water with dye was used, requiring only 5 mL of the reactive agent used as an accelerator for the reaction ($FeSO_4$ in acid solution). However, upon extrapolating the values for 1 m^3, it would be necessary to use 20 L of catalyst, ~278 g of iron sulfate with an approximate cost of $60, 110 mL of sulfuric acid that would cost ~$2, and distilled water that would cost $10, which would give a total cost of ~$72.

By comparing these data with those reported in Table 2, we found that the highest cost for the treatment would be the consumption of chemical reagents and not the electrical consumption, which makes the use of plasma more convenient as an effective treatment for elimination of organic contaminants compared to the Fenton or photo-Fenton process, among others, where a greater amount of chemical reagents is used and the efficiency in the degradation of dyes is similar [8].

Table 2
Electrical costs (USD per cubic meter of water treatment)

Treatment time (min)	Energy consumption (kWh/m^3)	Electrical costs (USD/m^3)
15	8	0.32
30	16	0.64
60	32	1.28
90	48	1.92
150	80	3.2

4. Conclusions

The efficiency of treatment with plasma and iron filings for DO39 dye removal was demonstrated, and after 45 min, the percentage of dye mineralization was greater than 50%, which allowed us to propose the serial combination of plasma treatment with another efficient treatment at lower dye concentrations. The absorbance reduction was 94.2% after 120 min, and the COD was 98.6% and TOC was 98.7%. The percentage of mineralization was 98.5% after 150 min of treatment. These results indicate that the use of iron filings as a catalyst accelerates the degradation process and facilitates the mineralization of the colorant. The concentrations of nitrates and nitrites were 214 and 32 mg/L, respectively, after 150 min. These values indicate that Plasma generates a significant number of nitrates and nitrites in the water, which would allow the treated water to be used in any agricultural application. From the optical spectrum of plasma emission, different species were identified (e.g., OH, N_2, Na, H_α, and H_β). The OES revealed that the presence of the catalyst increased the $^{\bullet}OH$ production, which favored the dye degradation and reduces the necessary treatment time. The G_{50} value was 0.825 g/kWh, this result is acceptable considering the values obtained in the degradation of this colorant by other processes; the electrical cost calculated for the treatment of 1 m^3 of water with this colorant using plasma was found to be $3.20 for 150 min of treatment, which, compared to other advanced processes, is a lower cost, these costs would allow this method to be used in the mineralization of organic compounds in larger volumes.

Acknowledgments

This research was supported by DGAPA IN105519, PRODEP DSA/103.5/15/6986, PROMEP 103.5/13/6626, PRODEP CA-5511-6/18-8304, PII-43/PIDE/2013, CONACyT 268644, and UAEM 4307/2017/CI.

References

[1] M. Rahimpour, H. Taghvaei, S. Zafarnak, M.R. Rahimpour, S. Raeissi, Post-discharge DBD plasma treatment for degradation of organic dye in water: a comparison with different plasma operation methods, J. Environ. Chem. Eng., 7 (2019) 103220 (1–10), doi: 10.1016/j.jece.2019.103220.

[2] P. Attri, M. Yusupov, J.H. Park, L.P. Lingamdinne, J.R. Koduru, M. Shiratani, E.H. Choi, A. Bogaerts, Mechanism and comparison of needle-type non-thermal direct and indirect atmospheric pressure plasma jets on the degradation of dyes, Sci. Rep., 6 (2016) 34419 (1–14), doi: 10.1038/srep34419.

[3] J. Xing-long, W. Xiao-yan, W. Qing-feng, Y. Jun-jie, C. Ya-qi, Plasma degradation of Cationic Blue dye with contact glow discharge electrolysis, Water Sci. Technol., 7 (2010) 1457–1463.

[4] M. Kadhom, N. Albayati, H. Alalwan, M. Al-Furaiji, Removal of dyes by agricultural waste, Sustainable Chem. Pharm., 16 (2020) 100259 (1–9), doi: 10.1016/j.scp.2020.100259.

[5] H. Ghodbane, O. Hamdaoui, J. Vandamme, J.V. Durme, P. Vanraes, C. Leys, A.Y. Nikiforov, Degradation of AB25 dye in liquid medium by atmospheric pressure non-thermal plasma and plasma combination with photocatalyst TiO_2, Open Chem., 13 (2015) 325–331.

[6] B. Acevedo, R.P. Rocha, M.F.R. Pereira, J.L. Figueiredo, C. Barriocanal, Adsorption of dyes by ACs prepared from waste tyre reinforcing fibre. Effect of texture, surface chemistry and pH, J. Colloid Interface Sci., 459 (2015) 189–198.

[7] K. Chen, L. Lin, Ch. F. Wang, M. Hwang, Interactions between new multi-anionic surfactants and direct dyes and their effects on the dyeing of cotton fabrics, Colloids Surf., A, 356 (2010) 46–50.

[8] C.L. Hsueh, Y.H. Huang, C.C. Wang, C.Y. Chen, Degradation of azo dyes using low iron concentration of Fenton and Fenton-like system, Chemosphere, 58 (2005) 1409–1414.

[9] A. Muniyasamy, G. Sivaporul, A. Gopinath, R. Lakshmanan, A. Altaee, A. Achary, P.V. Chellam, Process development for the degradation of textile azo dyes (mono-, di-, poly-) by advanced oxidation process - ozonation: experimental & partial derivative modelling approach, J. Environ. Manage., 265 (2020) 110397 (1–10), doi: 10.1016/j.jenvman.2020.110397.

[10] C.G. Silva, W. Wang, J.L. Faria, Photocatalytic and photochemical degradation of mono-, di- and tri-azo dyes in aqueous solution under UV irradiation, J. Photochem. Photobiol., A, 181 (2006) 314–324.

[11] R. Li, X. Song, Y. Huang, Y. Fang, M. Jia, W. Ma, Visible-light photocatalytic degradation of azo dyes in water by Ag_3PO_4: an unusual dependency between adsorption and the degradation rate on pH value, J. Mol. Catal. A: Chem., 421 (2016) 57–65.

[12] Y. Pan, Y. Wang, A. Zhou, A. Wang, Z. Wu, L. Lv, X. Li, K. Zhang, T. Zhu, Removal of azo dye in an up-flow membrane-less bioelectrochemical system integrated with bio-contact oxidation reactor, Chem. Eng. J., 326 (2017) 454–461.

[13] P.J. Quinlan, A. Tanvira, K.C. Tam, Application of the central composite design to study the flocculation of an anionic azo dye using quaternized cellulose nanofibrils, Carbohydr. Polym., 133 (2015) 80–89.

[14] X. Li, T. Wang, G. Qu, D. Liang, S. Hu, Enhanced degradation of azo dye in wastewater by pulsed discharge plasma coupled with MWCNTs-TiO_2/γ-Al_2O_3 composite photocatalyst, J. Environ. Manage., 172 (2016) 186–192.

[15] T.R. Waghmode, M.B. Kurade, R.T. Sapkal, C.H. Bhosale, B. Jeon, S.P. Govindwar, Sequential photocatalysis and biological treatment for the enhanced degradation of the persistent azo dye methyl red, J. Hazard. Mater., 371 (2019) 115–122.

[16] D. Vujevic, N. Koprivanac, A. Loncaric Bozic, B.R. Locke, The removal of Direct Orange 39 by pulsed corona discharge from model wastewater, Environ. Technol., 25 (2004) 791–800.

[17] Z.H. Qi, L. Yang, Y. Xia, Z.F. Ding, J.H. Niu, D.P. Liu, Y. Zhao, L.F. Ji, Y. Song, X. Song Lin, Removal of dimethyl phthalate in water by nonthermal air plasma treatment, Environ. Sci. Water Res. Technol., 5 (2019) 920–930.

[18] J.H. Park, N. Kumar, D.H. Park, M. Yusupov, E.C. Neyts, C.C.W. Verlackt, A. Bogaerts, M.H. Kang, H.S. Uhm, E.H. Choi, P. Attri, A comparative study for the inactivation of multidrug resistance bacteria using dielectric barrier discharge and nano-second pulsed plasma, Sci. Rep., 5 (2015) 1–14.

[19] X.J. Dai, C.S. Corr, S.B. Ponraj, M. Maniruzzaman, A.T. Ambujakshan, Z. Chen, L. Kviz, R. Lovett, G.D. Rajmohan, D.R. de Celis, M.L. Wright, P.R. Lamb, Y.E. Krasik, D.B. Graves, W.G. Graham, R. d'Agostino, X. Wang, Efficient and selectable production of reactive species using a nanosecond pulsed discharge in gas bubbles in liquid, Plasma Process. Polym., 13 (2016) 306–310.

[20] L.A.S.J. Carvalho, R.A. Konzen, A.C.M. Cunha, P.R. Batista, F.J. Bassetti, L.A. Coral, Efficiency of activated carbons and natural bentonite to remove direct orange 39 from water, J. Environ. Chem. Eng., 7 (2019) 103496 (1–11), doi: 10.1016/j.jece.2019.103496.

[21] Z.M. Fard, M. Bagheri, S. Rabieh, H.Z. Mousavi, Synthesis of hierarchical RGO@Cu_2O@Cu nanocomposites: optimization of photocatalytic degradation of Direct Orange 39 using a response surface methodology, J. Mater. Sci. - Mater. Electron., 13 (2017) 1–9.

[22] M. Muruganandham, J. Yang, J.J. Wu, Effect of ultrasonic irradiation on the catalytic activity and stability of goethite catalyst in the presence of H_2O_2 at acidic medium, Ind. Eng. Chem. Res., 46 (2007) 691–698.

[23] A.T. Sugiarto, S. Ito, T. Ohshima, M. Sato, J.D. Skalny, Oxidative decoloration of dyes by pulsed discharge plasma in water, J. Electrostat., 58 (2003) 135–145.

[24] P.M.K. Reddy, B. Ramaraju, C. Subrahmanyam, Degradation of malachite green by dielectric barrier discharge plasma, Water Sci. Technol., 67 (2013) 1097–1104.

[25] M.A. Malik, Water purification by plasmas: which reactors are most energy efficient?, Plasma Chem. Plasma Process., 30 (2010) 21–31.

[26] G.G. Raju, Collision cross sections in gaseous electronics part I: what do they mean?, IEEE Electr. Insul. Mag., 22 (2006) 5–23.

[27] Available at: https://www.nist.gov/

[28] V.K. Unnikrishnan, K. Alti, V.B. Kartha, C. Santhosh, G.P. Gupta, B.M. Suri, Measurements of plasma temperature and electron density in laser-induced copper plasma by time-resolved spectroscopy of neutral atom and ion emissions, Pramana J. Phys., 74 (2010) 983–993.

[29] H.R. Griem, Principles of Plasma Spectroscopy, Cambridge University Press, United Kingdom, 1997, 273 p.

[30] J. Feng, Z. Wang, Z. Li, W. Ni, Study to reduce laser induced breakdown spectroscopy measurement uncertainty using plasma characteristic parameters, Spectrochim. Acta, Part B, 65 (2010) 549–556.

[31] J. Vergara, C. Torres, E. Montiel, A. Gómez, P.G. Reyes, H. Martinez, Degradation of Textile Dye AB 52 in an aqueous solution by applying a plasma at atmospheric pressure, IEEE Trans. Plasma Sci., 45 (2017) 479–484.

[32] R. Zhou, R. Zhou, X. Zhang, J. Zhuang, S. Yang, K. Bazaka, K. Ostrikov, Effects of atmospheric-pressure N_2, He, air, and O_2 microplasmas on mung bean seed germination and seedling growth, Sci. Rep., 6 (2016) 1–11.

[33] B. Jiang, J. Zheng, S. Qiu, M. Wu, Q. Zhang, Z. Yan, Q. Xue, Review on electrical discharge plasma technology for wastewater remediation, Chem. Eng. J., 236 (2014) 348–368.

[34] I. Prasertsung, S. Kaewcharoen, K. Kunpinit, W. Yaowarat, N. Saito, T. Phenrat, Enhanced degradation of methylene blue by a solution plasma process catalyzed by incidentally co-generated copper nanoparticles, Water Sci. Technol., 79 (2019) 967–974.

[35] X. Wang, M. Zhou, X. Jin, Application of glow discharge plasma for wastewater treatment, Electrochim. Acta, 83 (2012) 501–512.
[36] M.A. Malik, A. Ghaffar, S.A. Malik, Water purification by electrical discharges, Plasma Sources Sci. Technol., 10 (2001) 82–91.
[37] K. Chen, J. Wu, C. Huang, Y. Liang, S.J. Hwang, Decolorization of azo dye using PVA-immobilized microorganisms, J. Biotechnol., 101 (2003) 241–252.
[38] H. Barrera, J. Cruz-Olivares, B.A. Frontana-Uribe, A. Gómez-Díaz, P.G. Reyes-Romero, C.E. Barrera-Diaz, Electro-oxidation–plasma treatment for azo dye carmoisine (Acid Red 14) in an aqueous solution, Materials, 13 (2020) 1–17.
[39] L. Sivachandiran and A. Khacef, Enhanced seed germination and plant growth by atmospheric pressure cold air plasma: combined effect of seed and water treatment, RSC Adv., 7 (2017) 1822–1832.
[40] D. Ghosh, C.R. Medhi, H. Solanki, M. K. Purkait, Decolorization of crystal violet solution by electrocoagulation, J. Environ. Prot. Sci., 2 (2008) 25–35.